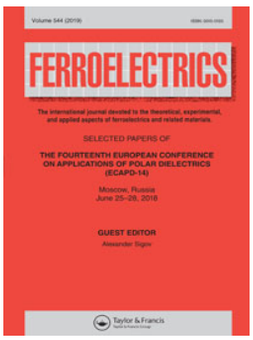

Ferroelectrics

ISSN: 0015-0193 (Print) 1563-5112 (Online) Journal homepage: https://www.tandfonline.com/loi/gfer20

Electronic and elastic properties of the multiferroic crystals with the Kagome type lattices -$Mn_3V_2O_8$ and $Ni_3V_2O_8$: First principle calculations

Husnu Koc, Selami Palaz, Amirullah M. Mamedov & Ekmel Ozbay

To cite this article: Husnu Koc, Selami Palaz, Amirullah M. Mamedov & Ekmel Ozbay (2019) Electronic and elastic properties of the multiferroic crystals with the Kagome type lattices -$Mn_3V_2O_8$ and $Ni_3V_2O_8$: First principle calculations, Ferroelectrics, 544:1, 11-19, DOI: 10.1080/00150193.2019.1598178

To link to this article: https://doi.org/10.1080/00150193.2019.1598178

Published online: 16 Aug 2019.

FERROELECTRICS
2019, VOL. 544, 11–19
https://doi.org/10.1080/00150193.2019.1598178

Taylor & Francis
Taylor & Francis Group

Electronic and elastic properties of the multiferroic crystals with the Kagome type lattices -$Mn_3V_2O_8$ and $Ni_3V_2O_8$: First principle calculations

Husnu Koc[a], Selami Palaz[b], Amirullah M. Mamedov[c,d], and Ekmel Ozbay[c]

[a]Faculty of Science and Letters, Department of Physics, Siirt University, Siirt, Turkey; [b]Faculty of Sciences, Department of Physics, Harran University, Sanliurfa, Turkey; [c]Nanotechnology Research Center, Bilkent University, Bilkent, Ankara, Turkey; [d]International Scientific Center, Baku State University, Baku, Azerbaijan

ABSTRACT

The electronic, mechanical, and optical properties of the Kagome staircase compounds, $Mn_3V_2O_8$ and $Ni_3V_2O_8$, have been investigated using the VASP (Vienna ab-initio Simulation Program) that was developed within the density functional theory (DFT). The spin polarized generalized gradient approximation has been used for modeling exchange-correlation effects. The electronic band structures for both compounds and total and partial density of states corresponding to these band structures have been calculated. Spin up (spin down) E_g values for $Mn_3V_2O_8$ and $Ni_3V_2O_8$ compounds are 0.77 eV indirect (3.18 direct) and 1.58 eV indirect (0.62 eV) direct, respectively. The band gaps of both compound is in the d-d character. Bulk modulus, shear modulus, Young's modulus, Poisson's ratio, anisotropic factors, sound velocity, and Debye temperature were calculated and interpreted.

ARTICLE HISTORY
Received 25 June 2018
Accepted 23 December 2018

KEYWORDS
Ab-initio calculation; Structural properties; Mechanical properties; Electronic properties

1. Introduction

The geometrically frustrated multiferroic $X_3V_2O_8$ (X = Mn, Ni, Co) compounds have a Kagome staircase system with a rich magnetic phase diagram due to a large number of different magnetic interactions. There are four ferroic orders (ferromagnetic, ferroelectric, ferroelastic, and ferrotoroidic) characterized by the formation of domes and exhibiting hysteresis behavior [1]. The multiferroic materials exhibit two or more ferroic orders. The studies on multiferroic Kagome staircase compounds have shown that there is a significant coupling between spin, lattice and charge degress of freedom. Each of the compounds $X_3V_2O_8$, which is a member of the quasi-isostructural, has slightly different spin -orbit coupling and magnetic anisotropies [2]. The compounds $Mn_3V_2O_8$ at the studies done up to now crystallize in two modifications depending on the temperature. It exhibits tetragonal structure (Space group $I4^-2d$) at high temperature while the $Mn_3V_2O_8$ compound exhibits orthorhombic (Space group Cmca) structure at low temperature [3]. The orthorhombic $Mn_3V_2O_8$ (MVO) compound is isostructural with

CONTACT Husnu Koc husnu_01_12@hotmail.com
Color versions of one or more of the figures in the article can be found online at www.tandfonline.com/gfer.

$Co_3V_2O_3$ (CVO) and $Ni_3V_2O_8$ (NVO) compounds. The $X_3V_2O_8$ (X = Mn, Ni, Co) compounds consist of layers of edge-sharing $X^{2+}O_6$ octahedra separated by $V^{5+}O_4$ tetrahedra [2, 4].

For MVO, two separate magnetic phase transitions have observed for the fields applied in the a, b, c crystallographic directions at 21 K and 15 K, respectively. A phase transition that appears to be specific heat but not seen in magnetization is found for all of the applied field orientations in the crystallographic directions, converging towards the 15 K transition as H→0. The magnetic behavior of MVO has critical fields for magnetic phase boundaries when the magnetic field is applied perpendicular to the Kagome staircase plane. The magnetic phase diagrams of the MVO compound are distinctly different from those observed for CVO and NVO [5]. According to the neutron scattering data, the CVO compound undergoes transition from paramagnetic state to a incommensurate antiferromagnetic state at 11.3 K. Also, It has been reported that the CVO compound has two incommensurate and one commensurate antiferromagnetic states between 11.3 K and 6.2 K, while transition from the antiferromagnetic state to the weakly ferromagnetic state at 6.2 K. NVO shows a different H-T diagram than the CVO compound. The magnetic properties of the NVO compound at S = 1 are less anisotropic. The NVO compound, which is tightly coupled to the magnetic properties, has a spontaneous polarization induced by the incommensurate magnetic order [2].

We discussed in this article the some of the previous studies on $X_3V_2O_8$ compounds. Javerock et al.[4] experimentally examined the structural characterization and optical properties of the $Ni_3V_2O_8$ and $Co_3V_2O_8$ compounds, and performed a comparison of the results of experimentally obtained XES and XAS data and PDOS data obtained with the first principle method. Clemens et al. [3] made a detailed analysis of the magnetic structure of the magnetic phase of the Mn3V2O8 compound with orthorhombic Kagome staircase structure at low temperature by the powder neutron diffraction method, and also performed PDOS calculations of $Mn_3V_2O_8$, $Ni_3V_2O_8$ and $Co_3V_2O_8$ compounds using the DFT + U method. Rai et al. [2] examined the optical and PDOS properties of the Kagome staircase $Co_3V_2O_8$ and $Ni_3V_2O_8$ compounds using the LDA + U method. Wang et al. [6] performed band structure and DOS calculations of $M_3V_2O_8$ (M = Mg, Ni, Zn) compounds with DFT calculations, but did not use spin polarization in calculations. In this study, our purpose is to investigate in detail the structural, electronic and mechanical properties of $Mn_3V_2O_8$ and $Ni_2V_2O_8$ compounds by DFT method. As far as we know, the electronic band structures along high symmetry directions and mechanical properties of these compounds have not been reported so far.

2. Method of calculation

In all of our calculations that were performed using the ab-initio total-energy and molecular-dynamics program VASP (Vienna ab-initio simulation program) [7–10] that was developed within the density functional theory (DFT) [11], the exchange-correlation energy function is treated within the a spin polarized GGA (generalized gradient approximation) by the density functional of Perdew et al. [12]. The potentials used for the GGA calculations take into account the $3p^6 3d^3 4s^2$ valence electrons of each V-,

$3p^6 3d^5 4s^2$ valence electrons of each Mn-, $3p^6 3d^8 4s^2$ valence electrons of each Ni-, and $2s^2 2p^4$ valence electrons of each O- atoms . When including a plane-wave basis up to a kinetic-energy cutoff equal to 19.55 Ha for $Mn_3V_2O_8$ and $V_2Ni_3O_8$, the properties investigated in this work are well converged. The Brillouin-zone integration was performed using special k points sampled within the Monkhorst-Pack scheme [13]. We found that a mesh of 5 x 5 x 4 k points and 6x6x4 k point for $Mn_3V_2O_8$ and $V_2Ni_3O_8$, respectively was required to describe the structural, mechanical, electronic properties. This k-point mesh guarantees a violation of charge neutrality less than 0.008e. Such a low value is a good indicator for an adequate convergence of the calculations.

3. Result and discussion

The $Mn_3V_2O_8$ and $Ni_3V_2O_8$ compounds belong to 64 (Cmca) space groups in orthorhombic phase. There are 4 molecules (Z = 4) in the unit cell. In this case, the unit cell contains 52 atoms. The positions of the atoms in the primitive cell of $Mn_3V_2O_8$ and $Ni_3V_2O_8$ compounds are given in Table 1. In the calculations, structural optimization calculations are performed using experimental lattice parameters and atomic positions [14, 15]. The total energy values corresponding to different volume values in the volume optimization calculations were determined. The lowest energy state is the most stable state, and the volume corresponding to these energy values is the sought volume value. The volume values obtained for $Mn_3V_2O_8$ and $Ni_3V_2O_8$ are 620.95 $Å^3$ and 562.64 $Å^3$, respectively. The lattice values obtained as a result of the calculations are in good agreement with the experimental values [14–18] below 1% (see Table 2). The total magnetic moments obtained for $Mn_3V_2O_8$ and $Ni_3V_2O_8$ are 30.0 and 12.0, respectively.

Table 1. The experimental atomic positions used in calculations [14, 15].

Space grup: Cmca-orthorhombic							
Atomic positions		$Mn_3V_2O_8$			$Ni_3V_2O_8$		
Atom	Wyckoff	x	y	z	x	y	z
$Mn_1(Ni_1)$	4a	0	0	0	0	0	0
$Mn_2(Ni_2)$	8e	0.25	0.13726	0.25	0.25	0.131	0.25
V	8f	0	0.37981	0.12038	0	0.376	0.120
O_1	8f	0	0.2544	0.2255	0	0.249	0.233
O_2	8f	0	−0.0003	0.2486	0	0.001	0.241
O_3	16g	0.2775	0.1177	0.9959	0.263	0.121	0.005

Table 2. The calculated equilibrium lattice parameters (a, b, and c) together with the experimental values and total magnetic moment (μ, in μB/f.u.) for Mn3V2O8 and Ni3V2O8 compounds.

Material	a (Å)	b (Å)	c (Å)	V_0 ($Å^3$)	μ	Refs.
$Mn_3V_2O_8$	6.211	11.848	8.438	620.95	30.0	Present
	6.247	11.728	8.491	622.09		Exp. [14]
$Ni_3V_2O_8$	5.919	11.490	8.273	562.64	12.0	Present
	5.933	11.385	8.239	556.52		Exp. [15]
	5.930	11.387	8.239	556.34		Exp. [16]
	5.906	11.380	8.240	553.81		Exp. [17]
	5.936	11.420	8.240	558.58		Exp. [18]

Table 3. The calculated elastic constants (in GPa) for $Mn_3V_2O_8$ and $Ni_3V_2O_8$ compounds.

Material	Reference	C_{11}	C_{12}	C_{13}	C_{22}	C_{23}	C_{33}	C_{44}	C_{55}	C_{66}
$Mn_3V_2O_8$	Present	130.2	43.9	70.9	160.0	74.9	167.0	32.7	48.3	58.2
$Ni_3V_2O_8$	Present	223.2	91.3	99.3	200.8	81.6	212.2	56.2	57.3	63.0

The strain-stress technique developed by Page et al. [19], which is compatible with the VASP package program, is used to calculate the elastic constants of structures. There are 9 independent elastic constants in an orthorhombic structure and it is important to obtain these constants for the identification of other elastic data. The elastic constants obtained by using the strain-stress technique are given in Table 3. Unfortunately, there are no experimental and theoretical results to be compared with the obtained results. whether a compound is mechanically stable is determined by the Born stability condition [20, 21]. The mechanical stability conditions of a compound in the orthorhombic structure are

$$(C_{11} + C_{22} - 2C_{12}) > 0,\ \ (C_{11} + C_{33} - 2C_{13}) > 0\ \ (C_{22+}C_{33} - 2C_{23}) > 0$$
$$C_{11} > 0,\ \ C_{22} > 0,\ \ C_{33} > 0,\ \ C_{44} > 0,\ \ C_{55} > 0,\ \ C_{66}$$
$$(C_{11} + C_{22} + C_{33} + 2C_{12} + 2C_{13} + 2C_{23}) > 0$$

The elastic constants obtained show that these compounds are mechanically stable. The C_{11}, C_{22} and C_{33} constants show resistance to linear compression in the a-, b- and c- directions, respectively. The C_{11} constant at the $Mn_3V_2O_8$ compound is smaller than the C_{22} and C_{33} constants. In the $Ni_3V_2O_8$ compound, the C_{22} constant is smaller than the C_{11} and C_{33} constants. In this case, It is said that there is more compression in the a-direction in the $Mn_3V_2O_8$ compound and in the b-direction in the $Ni_3V_2O_8$ compound.

The bulk modulus, shear modulus, Young modulus and Poisson ratio, which are the elastic modulus of the structures, are calculated according to Voight (V), Reuss (R) and Hill (H) approach [22–24].The values obtained from the Hill approach are the average of the values obtained from Voight and Reuss approaches. The elastic moduli obtained from the calculations are given in Table 4. The calculated bulk moduli of $Mn_3V_2O_8$ and $Ni_3V_2O_8$ compounds are 91.3 and 130.8 GPa, respectively. The large bulk modulus indicates that the change in volume versus pressure of the compound is small. Here, the most resistant compound to compression is $Ni_3V_2O_8$. The shear modulus is a measure of the resistance of a material against elastic deformation and shear stress. The shear module of $Ni_3V_2O_8$ is larger than the shear module of $Mn_3V_2O_8$. If the material is stiff, the Young's modulus is high. Here, the highest Young's modulus belongs to the $Ni_3V_2O_8$ compound. The Poisson' ratio [25–27] gives us information about the bond structure of the solids. The Poisson's ratio is 0.1 and 0.25 for covalent and ionic materials, respectively. The Poisson's ratio for the $Mn_3V_2O_8$ compound is 0.29 while the Poisson's ratio for the $Ni_3V_2O_8$ compound is 0.30. Therefore, it is said that the ionic bond is dominant for both compounds. It is determined by the ratio of B/G whether the materials are brittle or ductility). If B/G ratio is less (high) than 1.75, it is said that the material is brittle (ductility) [28, 29]. In this case, both of these compounds are ductile.

The anisotropic factors, Debye temperature and sound velocities [30–32] of these compounds are given in Table 5. The Debye temperature is high for soft materials,

Table 4. The calculated isotropic bulk modulus (B, in GPa), shear modulus (G, in GPa), Young's modulus (E, in GPa) and Poisson's ratio for $Mn_3V_2O_8$ and $Ni_3V_2O_8$ compounds.

Material	Reference	B_R	B_V	B_H	G_R	G_V	G_H	E	υ	G/B	B/G
$Mn_3V_2O_8$	Present	89.7	93.0	91.3	43.2	45.7	44.5	114.8	0.29	0.49	2.05
$Ni_3V_2O_8$	Present	130.4	131.2	130.8	59.4	59.6	59.5	155.0	0.30	0.46	2.20

Table 5. The calculated anisotropic factors, sound velocities (υ_t, υ_l, υ_m) , the Debye temperatures for $Mn_3V_2O_8$ and $Ni_3V_2O_8$ compounds.

Material	Reference	A_1	A_2	A_3	A_{comp}(%)	A_{shear}(%)	v_t	v_l	v_m	θ_D
$Mn_3V_2O_8$	Present	0.841	1.090	1.151	1.811	2.620	3246	5974	3622	472
$Ni_3V_2O_8$	Present	0.949	0.918	1.044	0.283	0.161	3523	6622	3937	530

small for hard materials. When Debye temperature values are taken into consideration, it can be said that these compounds are hard materials. But the $Ni_3V_2O_8$ from these compounds is harder than the $Mn_3V_2O_8$ compound. The shear anisotropic factors of orthorhombic compounds are given as $A_1=4C_{44}/C_{11}+C_{33}\text{-}2C_{13}$ for the {100} plane, $A_2=4C_{55}/C_{22}+C_{33}\text{-}2C_{23}$ for the {010} plane, and $A_3=4C_{66}/C_{11}+C_{22}\text{-}2C_{12}$ for the {001} plane. If the anisotropy factor is less than one, the greatest stiffness is in the <100> orientation, while in the case of greatness it is in the <111> orientation [33]. Among the anisotropy factors of the $Mn_3V_2O_8$ compound According to calculations made, A_1 is less than 1, A_2 is closer to 1, and A_3 is greater than 1. In the $Ni_3V_2O_8$ compound, A_1 and A_2 are small than 1, A_3 is closer to 1. The A_{comp} and A_{shear} anisotropy percentage [33] is another way of measuring elastic anisotropy. 0% value indicates elastic isotropic, 100% value indicates maximum elastic anisotropy. The A_{comp} and A_{shear} calculated for the $Mn_3V_2O_8$ compound are larger than the $Ni_3V_2O_8$ compound.

The spin up and spin down electronic band curves calculated for the $Mn_3V_2O_8$ and $Ni_3V_2O_8$ compounds in the orthorhombic structure and the total and partial density of states corresponding to these band curves are given in Figures 1–3. The spin polarized E_g value obtained for $Mn_3V_2O_8$ compound is 0.5 eV direct (Γ point). The Eg band gap is in the d-d character. As can be seen from Figures 1a and 2, the calculated spin up E_g values for $Mn_3V_2O_8$ compound is 0.77 eV indirect. while the maximum valence bands are localized at Γ, the least conduction bands have been localized at almost midpoint between Γ and S. In the valence bands occupied just below the Fermi level (zero eV), there is very weak O p and Mn d hybridization but the Mn d states are dominant. In the unoccupied conduction bands just above the Fermi level, V d states are dominant. The band gap obtained for spin down is Eg =3.18 eV direct (Γ point). $Mn_3V_2O_8$ compound in spin down exhibits insulator behavior. This is probably due to the fact that the O p states in the valence band energy region near the Fermi level resulting from the spin polarization included in the calculations are pushed further down and the Mn d states are pulled upward. The O p states in the occupied valence band just below the Fermi level are dominate while the V d + Mn d states in the unoccupied conduction bands just above the Fermi level are dominate. The spin polarized E_g=0.37 eV direct (Γ point) obtained for the $Mn_3V_2O_8$ compound is in agreement with the E_g=0.3 eV value obtained by Rai et al [34]. It is understood that both compounds from the calculated Eg value are narrow semiconductors in nature. As in the case of the $Mn_3V_2O_8$ compound, the band gap of this compound is also in the d-d character. The obtained spin up Eg

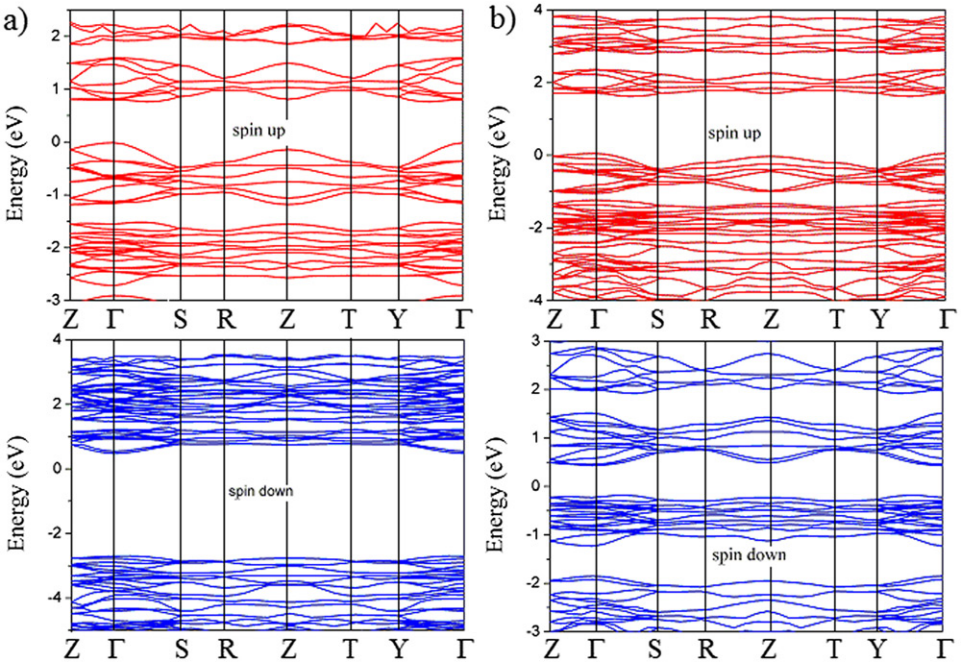

Figure 1. The calculated electronic band structures for the spin up and spin down of a)$Mn_3V_2O_8$ and b) $Ni_3V_2O_8$ compounds.

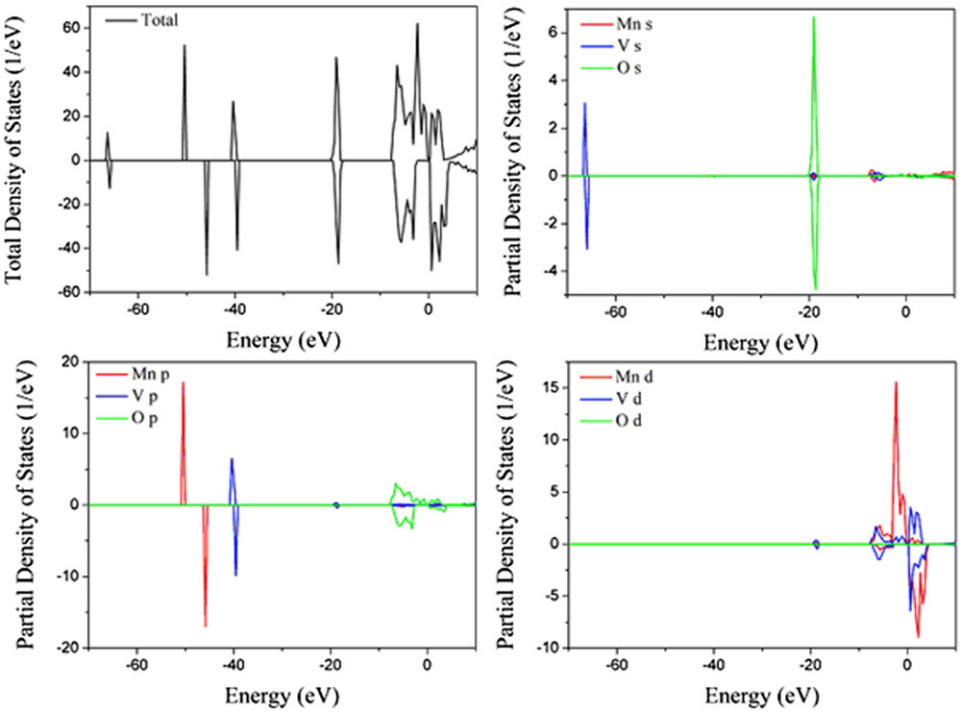

Figure 2. The spin-polarized total and projected density of states for $Mn_3V_2O_8$ compound.

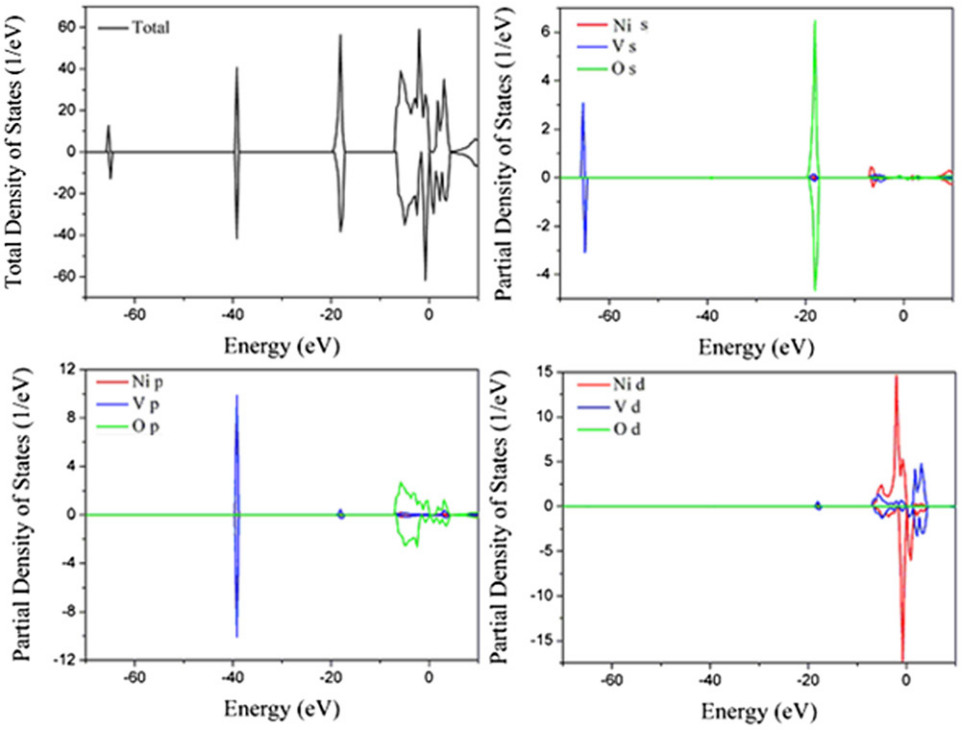

Figure 3. The spin-polarized total and projected density of states for $Ni_3V_2O_8$ compound.

for $Ni_3V_2O_8$ compound (Figure 1b) is 1.58 eV indirect ($E_V \rightarrow \Gamma$ point, $E_c \rightarrow$ almost midway between Γ and S) and the obtained spin down Eg is 0.62 eV indirect ($E_V \rightarrow$ almost midway between Γ and Y, $E_c \rightarrow \Gamma$ point). As can be seen in Figure 3, the valence bands at bottom in the -8-0 eV energy range are dominated by O p states, while the valence bands at the top are dominated by the Ni d states. The unoccupied conduction bands d in the lowest energy range are dominated by Ni d + V d states. The Eg (1.58 eV) value we calculated for spin up is in agreement with 1.3 eV value calculated by Wang et al.[6], but the E_g= 0.62 eV value we find for spin down is much smaller than 1.3. Probably, the spin polarization included in the calculations must have pushed further down the O p states in the -8-0 eV energy range, must have pulled upward the Ni d and Ni d + V d states in this valence band and in the lowest conduction band, respectively. When we examine Figures 2 and 3, it is seen that the partial density of satates curves obtained for spin up and spin down are different. The different partial density of states curves show antiferromagnetic interaction. The difference of the peaks indicates that all spins are aligned as ferromagnetic.

4. Conclusion

We have investigated the structural, mechanical and electronic properties of $Mn_3V_2O_8$ and $Ni_3V_2O_8$ compounds using the spin polarized GGA approximation in the frame of density functional theory. The lattice parameters obtained as a result of the optimization process are in agreement with the experimental values. The calculated electronic band

curves and the total and partial intensity of the states corresponding to these band curves are explained in detail and compared with other theoretical studies. When we consider the value of Young's modulus, which is a measure of stiffness, we can say that $Ni_3V_2O_8$ is harder stiffness material than $Mn_3V_2O_8$. The ionic bond for both compounds from calculated Poisson's ratio is dominant. Since the B/G ratio is high than 1.75, these compounds are ductile. The Debye temperature is low for soft materials and high for rigid materials. The rigid order of these compounds: are $Ni_3V_2O_8$>$Mn_3V_2O_8$.

Funding

One of the authors (Ekmel Ozbay) acknowledges partial support from the Turkish Academy of Sciences.

References

[1] A. Kumarasiri, Effects of transition metal doping on multiferroic ordering in $Ni_3V_2O_8$ and $FeVO_4$. Wayne State University Dissertations, The degree of Doctor of Philosophy, Detroit, Michigan, 144 pp. 2012.

[2] R. C. Rai *et al.*, High-energy magnetodielectric effect in Kagome staircase materials, *Phys. Rev. B.* **76** (17), 174414 (2007).

[3] O. Clemens, J. Rohrer, and G. Néner, Magnetic structures of the low temperature phase of $Mn_3(VO_4)_2$– towards understanding magnetic ordering between adjacent Kagomé layers, *Dalton Trans.* **45** (1), 156 (2016). DOI: 10.1039/C5DT03141A.

[4] J. Laverock *et al.*, Electronic structure of the kagom_e staircase compounds $Ni_3V_2O_8$ and $Co_3V_2O_8$, *Phys. Rev. B.* **87** (12), 125133 (2013). DOI: 10.1103/PhysRevB.87.125133.

[5] E. Morosan, J. Fleitman, T. Klimczuk, and R. J. Cava, Rich magnetic phase diagram of the Kagome-staircase compound $Mn_3V_2O_8$, *Phys. Rev. B.* **76** (14), 144403 (2007). DOI: 10.1103/PhysRevB.76.144403.

[6] D. Wang, J. Tang, Z. Zou, and J. Ye, Photophysical and photocatalytic properties of a series of visible-light driven photocatalysts $M_3V_2O_8$ (Mg, Ni, Zn), *Chem. Mater.* **17** (20), 5177 (2005).

[7] G. Kresse, and J. Hafner, Ab initio molecular dynamics for liquid metals, *Phys. Rev. B.* **47** (1), 558 (1993). DOI: 10.1103/PhysRevB.47.558.

[8] G. Kresse, and J. Furthmüller, Ab-initio total energy calculations for metals and semiconductors using a plane-wave basis set, *Comp. Mater. Sci.* **6** (1), 15 (1996). DOI: 10.1016/0927-0256(96)00008-0.

[9] G. Kresse, and D. Joubert, From ultrasoft pseudopotentials to the projector augmented-wave method, *Phys. Rev. B.* **59** (3), 1758 (1999). DOI: 10.1103/PhysRevB.59.1758.

[10] G. Kresse, and J. Furthmüller, Efficient iterative schemes for ab initio total- energy calculations using a plane-wave basis set, *Phys. Rev. B.* **54** (16), 11169 (1996). DOI: 10.1103/PhysRevB.54.11169.

[11] P. Hohenberg, and W. Kohn, Inhomogeneous electron gas, *Phys. Rev.* **136** (3B), B864 (1964).

[12] J. P. Perdew, S. Burke, and M. Ernzerhof, Generalized gradient approximation made simple, *Phys. Rev. Lett.* **77** (18), 3865 (1996). DOI: 10.1103/PhysRevLett.77.3865.

[13] H. J. Monkhorst, and J. D. Pack, Special points for Brillouin-zone integrations, *Phys. Rev. B.* **13** (12), 5188 (1976). DOI: 10.1103/PhysRevB.13.5188.

[14] X. Wang *et al.*, Crystal growth, structure, and properties of manganese orthovanadate $Mn_3(VO_4)_2$, *Solid State Sci.* **2** (1), 99 (2000). DOI: 10.1016/S1293-2558(00)00104-7.

[15] J. Isasi, New MM'O_4 oxides derived from the rutile type: synthesis, structure and study of magnetic and electronic properties, *J. Alloys Cmpnds.* **322** (1–2), 89 (2001). DOI: 10.1016/S0925-8388(00)01495-X.
[16] R. R. George, D. S. Robert, and K. W. Robert, Origin of the yellow color of complex nickel oxides, *J. Solid State Chem.* **39**, 277 (1981).
[17] H. Feuss, E. F. Bertaut, R. Pauthenet, and A. Durif, Structure aux Rayons X, Neutrons et Propri6t6s Magn6tiqnes des Orthovanadates de Nickel et de Cobalt, *Acta Crystallogr. B Struct. Crystallogr. Cryst. Chem.* **26**, 2036 (1970). DOI: 10.1107/S0567740870005344.
[18] E. E. Sauerbrei, R. Faggiani, and C. Caluo, Refinement of the crystal structures of $Co_3V_2O_8$ and $Ni_3V_2O_8$, *Acta Crystallogr. B Struct. Sci.* **B29**, 2304 (1973). DOI: 10.1107/S0567740873006552.
[19] Y. L. Page, and P. Saxe, Symmetry-general least-squares extraction of elastic coefficients from ab initio total energy, *Phys. Rev. B.* **63**, 174103 (2001). DOI: 10.1103/PhysRevB.63.174103.
[20] O. Beckstein, J. E. Klepeis, G. L. W. Hart, and O. Pankratov, First-principles elastic constants and electronic structure of α-Pt_2Si and PtSi, *Phys. Rev. B.* **63** (13), 134112 (2001). DOI: 10.1103/PhysRevB.63.134112.
[21] D. C. Wallace, *Thermodynamics of Crystals* (New York: Wiley 1972).
[22] W. Voight, *Lehrbook der kristallphysik Leipsig* (Leipzig, Berlin: B.G. Teubner 1928: p. 962).
[23] A. Reuss, Berechnung der fließgrenze von mischkristallen auf grund der plastizitatsbedingung f ¨ ur einkristalle, *Z Angew. Math. Mech.* **9** (1), 49 (1929). DOI: 10.1002/zamm.19290090104.
[24] R. Hill, The elastic behavior of crystalline aggregate, *Proc. Phys. Soc. A.* **65** (5), 349 (1952). DOI: 10.1088/0370-1298/65/5/307.
[25] V. V. Bannikov, I. R. Shein, and A. L. Ivanovskii, Electronic structure, chemical bonding and elastic properties of the first thorium-containing nitride perovskite $TaThN_3$, *Phys. Stat. Sol. (RRL).* **3**, 89 (2007). DOI: 10.1002/pssr.200600116.
[26] H. Koc, A. Yildirim, E. Tetik, and E. Deligoz, Ab initio calculation of the structural, elastik, electronic, and linear optical properties of ZrPtSi and TiPtSi ternary compounds, *Comput. Mater. Sci.* **62**, 235 (2012). DOI: 10.1016/j.commatsci.2012.05.052.
[27] H. Koc, A. M. Mamedov, E. Deligoz, and H. Ozisik, First principles prediction of the elastic, electronic, and optical properties of Sb_2S_3 and Sb_2Se_3 compounds, *Solid State Sci.* **14** (8), 1211 (2012). DOI: 10.1016/j.solidstatesciences.2012.06.003.
[28] I. R. Shein, and A. L. Ivanovskii, Elastic properties of mono- and polycrystalline hexagonal AlB_2-like diborides of s, p and d metals from first-principles calculations, *J. Phys: Condens. Matter.* **20**, 415218.1 (2008). DOI: 10.1088/0953-8984/20/41/415218.
[29] F. Pogh, Relations between the elastic moduli and the plastic properties of polycrystalline pure metals, *Philos. Mag.* **45**, 823 (1954).
[30] I. Johnston, G. Keeler, R. Rollins, and S. Spicklemire, *Solids State Physics Simulations, the Consortium for Upper Level Physics Software* (Wiley, New York 1996).
[31] O. L. Anderson, A simplified method for calculating the Debye temperature from elastic constants, *J Phys Chem Solids.* **24** (7), 909 (1963). DOI: 10.1016/0022-3697(63)90067-2.
[32] E. Schreiber, O. L. Anderson, and N. Soga, *Elastic Constants and Their Measurements* (McGraw-Hill, New York 1973).
[33] D. H. Chung, and W. R. Buessem, *Anisotropy in Single Crystal Refractory Compounds*, edited by F. W. Vahldiek, S. A. Mersol (Plenum, New York 1968: p 217).
[34] R. C. Rai *et al.*, Optical properties and magnetic-field-induced phase transition in the ferroelectric state of $Ni_3V_2O_8$: Experiments and first-principles calculations, *Phys. Rev. B.* **74** (23), 235101 (2006). DOI: 10.1103/PhysRevB.74.235101.